Journal of Ultrafine Grained and Nanostructured Materials
https://jufgnsm.ut.ac.ir
Vol. 49, No.1, June 2016, pp. 22-28
Print ISSN: 2423-6845 Online ISSN: 2423-6837
DOI: 10.7508/jufgnsm.2016.01.04

Corrosion Behavior of Al-2wt%Cu Alloy Processed By Accumulative Roll Bonding (ARB) Process

Mohammad Abdolahi Sereshki[1], Bahram Azad[*2], Ehsan Borhani[3]

[1]Department of Materials Engineering, Science and Research Branch, Islamic Azad University, Tehran , Iran

[2]Faculty of Materials and Metallurgical Engineering, Semnan University, Semnan, Iran

[3]Department of Nanotechnology, Nano-Materials Science and Engineering group, Semnan University, Semnan, Iran

Recieved: 5 April 2016; Accepted: 28 May 2016

Corresponding author email: bahramazad1987@gmail.com

ABSTRACT

Accumulative roll bonding (ARB) imposes severe plastic strain on materials without changing the specimen dimensions. ARB process is mostly appropriate for practical applications because it can be performed readily by the conventional rolling process. An Al-2wt%Cu alloy was subjected to ARB process up to a strain of 4.8. Stacking of materials and conventional roll-bonding are repeated in the process. In this study, corrosion behavior of an Al-2wt%Cu alloy fabricated by ARB process was studied in 3.5%wtNaCl solution using potentiodynamic polarization and electrochemical impedance spectroscopy (EIS). The morphology of structures was analyzed by scanning electron microscopy with energy dispersive X-ray spectroscopy (SEM-EDX). Also, the electrochemical experiments showed that corrosion resistance of samples decreases with increasing the number of ARB cycles due to the formation of oxide layer on defects and energetic regions such as grain boundaries with low/high angle and high density dislocations accumulated in sub-grains. According to the nyquist curves, by continuing the process, the diameters of semicircles decreased and the corrosion resistance and the polarization resistance subsequently decreased. After 6-cycle ARB, link up of small pits and micro crack were seen. Also, with increasing the number of the ARB cycles, the mean grain size of specimens decreased and it reached to 650 nm after 6 cycles of ARB process.

Keywords: *Accumulative Roll Bonding (ARB); Al-2wt%Cu Alloy; Electrochemical Impedance Spectroscopy (EIS); Pitting Corrosion; Polarization.*

1. Introduction

Severe plastic deformation (SPD) techniques are now widely applied for the production of ultrafine-grained (UFG) microstructures in bulk metals with mean grain size smaller than 1 μm [1,2]. Several SPD methods such as equal channel angular pressing (ECAP) [3], high pressure torsion (HPT) [4], multi-axial compression/forging (MAC/F) [5], cyclic extrusion compression (CEC) [6] and accumulative roll bonding (ARB) [7,8], have been developed. Among these SPD techniques, ARB process allows to accumulate very large plastic strains into materials without changing the dimensions of materials by repeating the process of cutting the rolled sheet, stacking them to be the initial thickness and roll-bonding the stacked sheets again [7,8]. Microstructure evolution, mechanical properties and texture evolution of ARB-processed alloys have studied by many researchers [1,9-12], however, some characteristics of ARB-processed alloys such as corrosion behavior still need an in-

depth research. Naeini et al. [13] studied the pitting corrosion resistance of UFG AA-5052 processed by ARB process in 3.5% NaCl. They found that pitting corrosion resistance decreased with increasing the number of ARB cycles. Eizadjou et al.[14] investigated the pitting corrosion susceptibility of ARBed pure aluminum. They concluded that anodic breakdown and repassivation potentials decrease with increasing the number of ARB cycles. Korchef et al. [15] studied the corrosion behavior of pure aluminum processed by ECAP. They pointed out that corrosion resistance of the alloy decreases with increasing the number of ECAP cycles. Also, Akiyama et al. [16] reported the corrosion behavior of ECAP-processed Al-alloys in natural buffer solution containing 0.002 M NaCl. They found out that the pitting corrosion resistance was deteriorated.

In this study, the corrosion behavior of Al-2%Cu alloy processed by ARB process with potentiodynamic polarization an EIS tests in 3.5% NaCl solution was investigated, and the results compared to a solution-treated (ST) specimen.

2. Materials and Experimental Procedure

The chemical composition of the used material is as follow (wt%): 1.96Cu-0.001Mg-0.022Fe-0.004Si-0.001Mn-0.006Cr-0.0001Ti-Al (base). The used sheets for the experiments were solution-treated at 550°C/6hr and immediately quenched in the water. The samples were prepared with a thickness of 2 mm, a width of 60 mm and a length of 200 mm. Some of the ST sheets were firstly cold-rolled by 50% reduction in the thickness. To prepare of the sheets and create a satisfactory bond in the ARB process, the surfaces of the sheets were cleaned by acetone and were roughened by a wire brush. The ARB process was immediately carried out to avoid for any oxide formation.

The ARB process was carried out by two mills with 110 mm diameter rolls having rolling speed of 0.167 m/s. After the cold-rolling, the sheets were immediately quenched in the water. The sheets with 1 mm thickness were cut into half-length and then the sheets were stacked to be 2 mm and roll bonded by 50% reduction. These stages repeated up to 6 cycles.

All electrochemical experiments were performed in 3.5%NaCl solution at room temperature using a potentiostat model IVIUMSTAT. A saturated calomel electrode (SCE) and a Pt rod were used as reference and counter electrodes, respectively. The working electrodes were ST and ARBed specimens which they were ground up to 2000 grade with SiC paper, washed with distilled water and then degreased ultrasonically with acetone in 10 minutes and finally washed with distilled water again. In the case of polarization tests, after each cycles of ARB process, determination of open circuit potential (OCP), was carried out after 30 minutes immersion in NaCl solution and then tests were performed at scan rate of 1 mV/S. Furthermore, all electrochemical data and corrosion rates were extracted by Cview software, version 3.3.

3. Result and Discussion

In order to understand the effect of grain size on the corrosion behavior, the change in the grain size as a function of the number of ARB cycle is shown in Fig. 1 [7]. The grain size of the specimen decreases with increasing the number of ARB cycle and reaches to 650 nm after 6-cycle ARB process. The accumulation of shear deformation during ARB process is dominant driving force for the grain refinement and the grain subdivision.

Two different methods were used in order to evaluate the corrosion behavior of specimens as following:

3.1. Polarization tests

Figure 2 shows the polarization curves for ST and ARBed specimens. Table 1 lists the E_{Corr}, i_{Corr}, R_P and corrosion rate (C.R.) as a function of the number of ARB cycles. Also this result is schematically shown in Fig. 3. As shown in Fig. 3, the magnitude of C.R. for Annealed specimen (ST specimen) is lower than others. This clearly indicates that by increasing the number of ARB cycles, corrosion resistance of the samples decreases.

3.2. Electrochemical Impedance Spectroscopy (EIS)

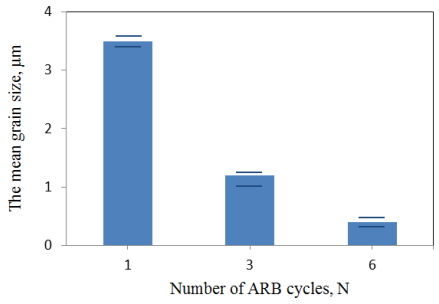

Fig. 1- Change in grain size as a function of the number of ARB cycles.

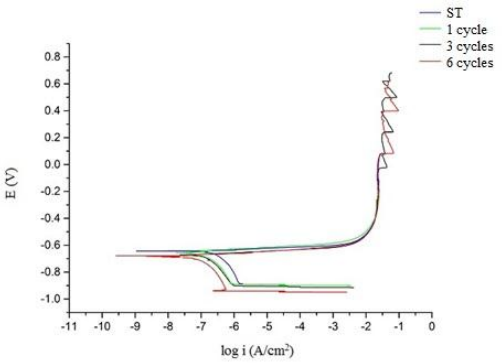

Fig. 2- Polarization curves for ST and ARBed samples in 3.5% NaCl Solution.

Table 1- Electrochemical data for ST and ARBed samples.

	C.R.(mpy)	I(A/cm²)	E(V)	R_p(Ω.cm²)
ST	0.030	7.16E-08	-0.686	**3.035E5**
1 cycle	0.065	1.51E-07	-0.658	**1.43E5**
3 cycles	0.087	2.04E-07	-0.676	**1.062E5**
6 cycles	0.118	2.70E-07	-0.644	**99221**

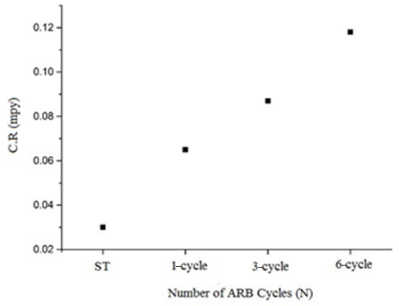

Fig. 3- Corrosion rate as a function of the number of ARB cycles.

Figure 4 shows the impedance spectra on nyquist plots obtained at OCP from the ST and ARBed specimens immersed into 3.5% NaCl solution. The results of EIS measurement show the diameter of semicircles, giving the polarization resistance (R_p). High R_p values indicate that a stable oxide layer were formed on the alloy and has an excellent corrosion resistance. As can be seen, with increasing the number of ARB cycles (N), the polarization resistance decreases. According to Stern-Gery equation, i_{corr} is inversely proportional to R_p [15]:

$$i_{Corr} = \frac{b_a b_c}{2.3\,(b_a+b_c)R_P} \quad (1)$$

where i_{Corr} is the corrosion current density, b_a and b_c are the anodic and cathodic Tafel coefficients, respectively, and R_p is the polarization resistance. On the other hand, with increasing the Cl^- ion, the charge-transfer resistance decreases, therefore, oxide layer breaks down and working electrode becomes less passive. In fact, with increasing the semicircle diameter, the electrode resistance against corrosive anion (Cl^-) increases. It should be noted that with increasing the number of ARB cycles, the diameters decreases, as a result, the corrosion resistance decreased.

An equivalent circuit (Randles Circuit) which is very common is shown in Fig. 5. As can be seen, the electrochemical system of metal/oxide layer/ electrolyte, where R_S, R_p and C represent the electrolyte resistance, the charge-transfer resistance and interfacial capacitance, respectively. This capacitance contains the contribution of the passive film C_f and the double layer C_{dl}, which are in series.

3.3. Surface Analysis

The SEM micrographs of all specimens are shown in Fig. 6. As shown in Fig. 6 (a), portray small pits that they distribute uniformly on the surface, after 1 cycle of ARB process, these pits increase and become deeper. Therefore, with increasing the number of ARB cycles, the number of pits increases.

It should be noted that, the pits in N=6 and N=3 are larger and deeper than the pits in N=1. On the

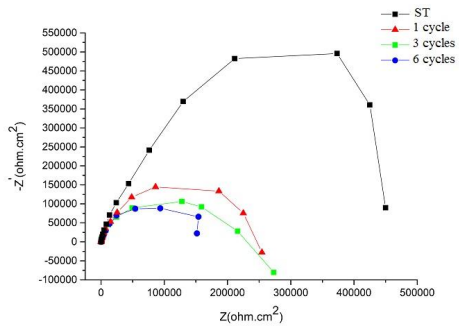

Fig. 4- Nyquist plot of ST and ARBed samples in 3.5% NaCl solution at room temperature.

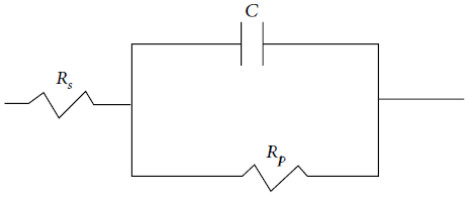

Fig. 5- Electrical equivalent circuit [15].

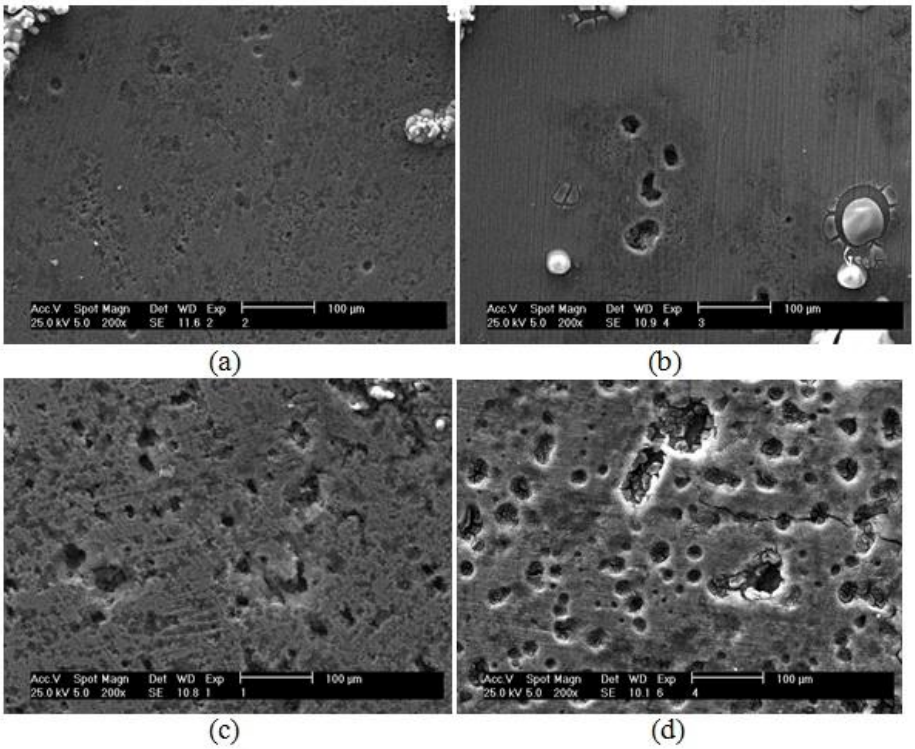

Fig. 6- SEM micrographs of ST and ARBed samples after electrochemical tests, (a) ST, (b) N=1, (c) N=3 and (d) N=6.

other hand, as shown in Fig. 6, in N=6, these pits link up to form larger pits and create micro cracks. The crack and links up of the pitting are shown by red arrows in Fig. 7.

The SEM micrographs with energy dispersive X-Ray (EDX) analysis were performed in the localized corrosion regions (pits) in order to investigate the type of existing elements and results are shown in Fig. 8. The analyzed pits are indicated by red arrow. Table 2 shows Cu remnants in pits in different cycles. Andreatta et al. [17] studied the effect of solution heat treatment on corrosion behavior between intermetallic (IM) and matrix in AA7075-T6. They reported that IM particles such as $MgZn_2$, dissolved during ST and matrix enriched by Zn and Mg. Al-2%wtCu alloy has some IM particles containing Cu. Therefore, as concluded above during ST, these particles dissolved and matrix enriched with Cu.

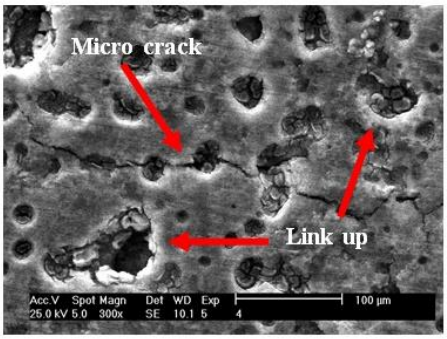

Fig. 7- SEM micrograph of ARBed sample after 6cycles.

As can be seen, Cu is one of the elements has remained in the pits. With increasing the number of ARB cycles, Cu remnant increases. The number of ARB cycles versus Cu remnants is shown in Fig. 9. This phenomenon requires further investigation to determine which factors cause to remaining Cu in the pits.

Localized corrosion attack on Al alloys in solution containing aggressive ion like Cl^- has been focus of many studies in the literature [18-22]. Except pure aluminum that its corrosion relates to properties of aluminum, in the case of aluminum alloys, corrosion relates to alloy composition, micro defects (such as vacancies, voids, etc.), macro defects (e.g. second phase particles, inclusions and etc.) and structure of the oxide film [22]. As previously mentioned in this study, the samples were solution treated and intermetallics have been made. It can be said that one of the most important factors to

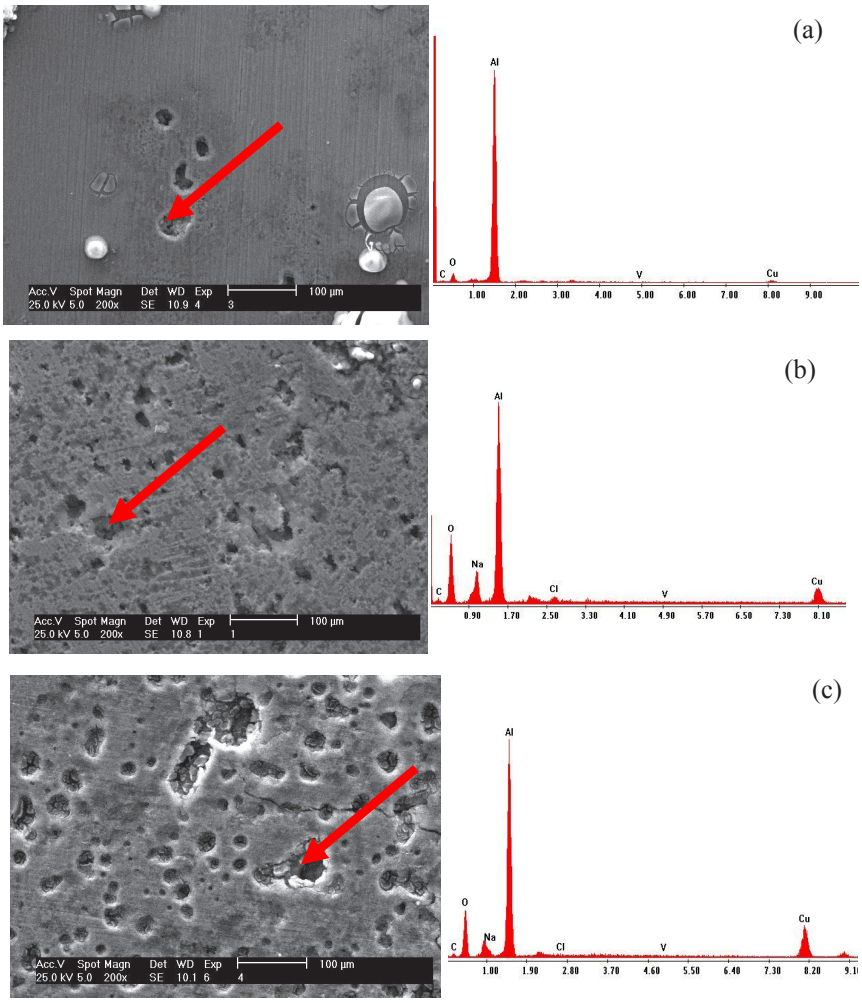

Fig. 8- SEM micrographs with EDX analysis in localized corrosion regions (pits) after electrochemical tests, (a) N=1, (b) N=3 and (c) N=6.

Table 2. Cu remnants (at%) in pits after electrochemical tests.

N	1	3	6
Cu remnants	1.29	4.16	8.57

increase corrosion susceptibility is the structure of the oxide film. Guillaumin et al. [19] found out that the volta potential of the surface of AA-2024-T3, not only relates to chemical composition, but also, relates to other parameters such as composition of the oxide film. Moreover, according to Szklarska-Smialowska [22], the pitting corrosion of Al and its alloys in halide containing solution, contains four stages, which are adsorption of Cl^- by oxide film, oxide layer breakdown and penetration of aggressive ion into it, formation of metastable pits, and finally the stable pit growth. Many studies based on different analytical techniques have proved this phenomenon [23-28]. In addition, the formation of subgrains with high dislocation densities and UFGs structures which are surrounded by sharp and strongly deformed boundaries [11] due to ARB process, are the other reasons to decrease corrosion resistance because the oxide film which forms on such high level energy and defectful substrate seem to have more defective structure. On the other hand, the increasing of the dislocation density due to severe plastic deformation could be one of the reasons for decreasing the corrosion resistance of the deformed Al alloy. This result is in agreement with study of Schultze et al. [20]. It can be concluded that the more defective oxide layer, the more susceptibility to pitting corrosion. The results obtained from electrochemical experiments

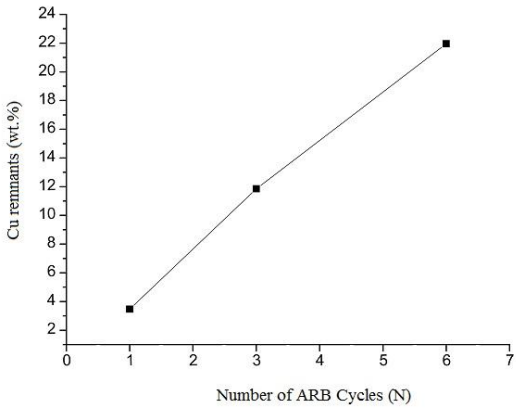

Fig. 9- The number of ARB cycles (N) VS. Cu remnants in pits after electrochemical tests in ARBed samples.

demonstrate that pitting corrosion resistance of Al-2wt%Cu decreases under influence of ARB process, mainly due to the formation of defectful oxide layer on defective substrate and also the increasing of density of the dislocations in the subgrains.

4. Conclusion

Polarization and Impedance methods were used in order to evaluate the corrosion behavior of specimens. Based on the results of this work, the following conclusions were obtained:

1. According to the polarization data, with increasing the number of ARB cycles from 1 to 6 cycles, the current density increased from 1.51E-07 to 2.70E-07 due to the formation defective oxide layer on the alloy's surface, therefore, the corrosion rate increased from 0.065 to 0.118.

2. According to the nyquist curves, with increasing the number of ARB cycles, the diameters of semicircles decreased, as a result, the corrosion resistance and the polarization resistance decreased.

3. In 0-cycle ARB process (before the ARB process), small pits that they distribute uniformly on the surface, after 1 cycle-ARB, these pits increased and became deeper. Therefore, the number of deeper and larger pits increased with increasing the number of ARB cycles.

4. Link up of small pits and micro crack were observed after 6 cycles of the ARB process.

5. Cu remnants were determined by EDX analyze and increased with increasing the number of ARB cycles. This phenomenon requires further investigation.

References

1. Borhani E, Jafarian H, Shibata A, Tsuji N. Texture Evolution in Al–0.2 mass% Sc Alloy during ARB Process and Subsequent Annealing. Materials Transactions. 2012;53(11):1863-9.

2. Valiev RZ, Estrin Y, Horita Z, Langdon TG, Zechetbauer MJ, Zhu YT. Producing bulk ultrafine-grained materials by severe plastic deformation. The Journal of The Minerals, Metals & Materials Society. 2006;58(4):33-9.

3. Valiev RZ, Langdon TG. Principles of equal-channel angular pressing as a processing tool for grain refinement. Progress in Materials Science. 2006;51(7):881-981.

4. Valiev RZ, Alexandrov IV. Nanostructured materials from severe plastic deformation. Nanostructured materials. 1999;12(1):35-40.

5. Cherukuri B, Nedkova TS, Srinivasan R. A comparison of the properties of SPD-processed AA-6061 by equal-channel angular pressing, multi-axial compressions/forgings and accumulative roll bonding. Materials Science and Engineering: A. 2005;410:394-7.

6. Richert M, Liu Q, Hansen N. Microstructural evolution over a large strain range in aluminium deformed by cyclic-extrusion–compression. Materials Science and Engineering: A. 1999;260(1):275-83.

7. Azad B, Borhani E. The Effect of Al2Cu Precipitate Size on Microstructure and Mechanical Properties of Al-2 wt.% Cu Alloys Fabricated by ARB. Journal of Materials Engineering and Performance. 2015;24(12):4789-96.

8. Azad B, Borhani E. Pre-aging time dependence of microstructure and mechanical properties in nanostructured Al-2wt% Cu alloy. Metals and Materials International. 2016;22(2):243-51.

9. Borhani E, Jafarian H, Adachi H, Terada D, Tsuji N. Annealing Behavior of Solution Treated and Aged Al-0.2 wt% Sc Deformed by ARB. InMaterials Science Forum. 2010;667:211-216.

10. Borhani E, Jafarian H, Sato T, Terada D, Miyajima N, Tsuji N. Proceeding 12th International Conference on Aluminum Alloys. 2010; Yokohama, Japan;2168-73.

11. Borhani E, Jafarian H, Terada D, Adachi H, Tsuji N. Microstructural Evolution during ARB Process of Al-0.2 mass% Sc Alloy Containing Al3Sc Precipitates in Starting Structures. Materials transactions. 2012;53(1):72-80.

12. Azad B, Borhani E. A study on the effect of nano-precipitates on fracture behavior of nano-structured Al-2wt% Cu alloy fabricated by accumulative roll bonding (ARB) process. Journal of Mining and Metallurgy, Section B: Metallurgy. 2016;52(1):93-98.

13. Naeini MF, Shariat MH, Eizadjou M. On the chloride-induced pitting of ultra fine grains 5052 aluminum alloy produced by accumulative roll bonding process. Journal of Alloys and Compounds. 2011;509(14):4696-700.

14. Eizadjou M, Fattahi H, Talachi AK, Manesh HD, Janghorban K, Shariat MH. Pitting corrosion susceptibility of ultrafine grains commercially pure aluminium produced by accumulative roll bonding process. Corrosion Engineering, Science and Technology. 2012;47(1):19-24.

15. Korchef A, Kahoul A. Corrosion behavior of commercial aluminum alloy processed by equal channel angular pressing. International Journal of Corrosion. 2013;983261;doi: 10.1155/2013/983261.

16. Akiyama E, Zhang Z, Watanabe Y, Tsuzaki K. Effects of severe plastic deformation on the corrosion behavior of aluminum alloys. Journal of Solid State Electrochemistry. 2009;13(2):277-82.

17. Andreatta F, Terryn H, De Wit JH. Effect of solution heat treatment on galvanic coupling between intermetallics and matrix in AA7075-T6. Corrosion Science. 2003;45(8):1733-46.

18. Boag A, Hughes AE, Glenn AM, Muster TH, McCulloch D. Corrosion of AA2024-T3 Part I: Localised corrosion of isolated IM particles. Corrosion Science. 2011;53(1):17-26.

19. Guillaumin V, Schmutz P, Frankel GS. Characterization of corrosion interfaces by the scanning Kelvin probe force microscopy technique. Journal of the Electrochemical Society. 2001;148(5):B163-73.

20. Schultze JW, Davepon B, Karman F, Rosenkranz C, Schreiber A, Voigt O. Corrosion and passivation in nanoscopic and microscopic dimensions: the influence of grains and grain boundaries. Corrosion engineering, science and technology. 2004;39(1):45-52.

21. King PC, Cole IS, Corrigan PA, Hughes AE, Muster TH, Thomas S. FIB/SEM study of AA2024 corrosion under a seawater drop, part II. Corrosion Science. 2012;55:116-25.

22. Szklarska-Smialowska Z. Pitting corrosion of aluminum. Corrosion science. 1999;41(9):1743-67.

23. Augustynski J, Frankenthal RP, Kruger J. Proceeding 4th International Symposium on Passivity. 1978; Princeton, NJ, USA; The Electrochemical Society;997.

24. Berzins A, Evans JV, Lowson RT. Aluminium corrosion studies. II. Corrosion rates in water. Australian Journal of Chemistry. 1977;30(4):721-31.

25. Blanc C, Mankowski G. Susceptibility to pitting corrosion of 6056 aluminium alloy. Corrosion science. 1997;39(5):949-59.

26. Brunner JG, Birbilis N, Ralston KD, Virtanen S. Impact of ultrafine-grained microstructure on the corrosion of aluminium alloy AA2024. Corrosion Science. 2012;57:209-14.

27. DeRose JA, Suter T, Bałkowiec A, Michalski J, Kurzydlowski KJ, Schmutz P. Localised corrosion initiation and microstructural characterisation of an Al 2024 alloy with a higher Cu to Mg ratio. Corrosion Science. 2012;55:313-25.

28. Wood GC, Richardson JA, Abd Rabbo MF, Mapa LP, Sutton WH. Proceeding 4th International Symposium on Passivity. 1978; Princeton, NJ, USA; The Electrochemical Society;973.